

Microstructure and mechanical properties of bamboo in compression

by

Michael R. Gerhardt

Submitted to the  
Department of Materials Science and Engineering  
in Partial Fulfillment of the Requirements for the Degree of  
Bachelor of Science

at the

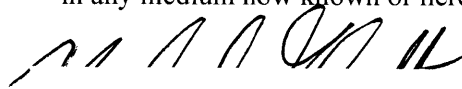
Massachusetts Institute of Technology

May 11, 2012

© 2012 Michael R. Gerhardt

All rights reserved

The author hereby grants to MIT permission to reproduce and to  
distribute publicly paper and electronic copies of this thesis document in whole or in part  
in any medium now known or hereafter created.



Signature of Author .....

Department of Materials Science and Engineering  
May 11, 2012

Certified by .....

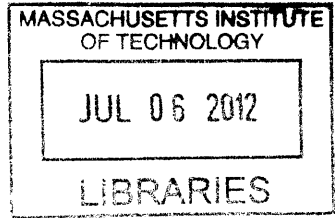
Lorna J. Gibson  
Matoula S. Salapatas Professor of Materials Science and Engineering  
Thesis Supervisor



Accepted by .....

Jeffrey C. Grossman  
Carl Richard Soderberg Associate Professor of Power Engineering  
Chairman, Undergraduate Committee

**ARCHIVES**



**Abstract**

Bamboo has received much interest recently as a construction material due to its strength, rapid growth, and abundance in developing nations such as China, India, and Brazil. The main obstacle to the widespread use of bamboo as a structural material is the lack of adequate information on the mechanical properties of bamboo. In this work, the microstructure and mechanical properties of *Phyllostachis dulcis* bamboo are studied to help produce a model for the mechanical properties of bamboo. Specifically, a linear relationship is established between the density of bamboo samples, which is known to vary radially, and their strength in compression. Nanoindentation of vascular bundles in various positions in bamboo samples revealed that the Young's modulus and hardness of the bundles vary in the radial direction but not around the circumference. The compressive strength of bamboo samples was found to vary from 40 to 95 MPa, while nanoindentation results show the Young's modulus of vascular bundles ranges from 15 to 18 GPa and the hardness ranges from 380 to 530 MPa.

**Table of Contents**

1. Introduction	pg. 5
1.1 Microstructure of bamboo	pg. 5
1.2 Modeling of bamboo as a cellular solid	pg. 7
2. Methods and Materials	pg. 11
2.1 Nanoindentation	pg. 11
2.2 Scanning electron microscopy	pg. 13
2.3 Microstructure analysis	pg. 14
2.4 Mechanical testing	pg. 14
3. Results and discussion	pg. 17
3.1 Nanoindentation	pg. 17
3.2 SEM micrographs and microstructure analysis	pg. 19
3.3 Mechanical testing	pg. 26
4. Conclusion	pg. 32
5. Acknowledgements	pg. 33
6. Works Cited	pg. 34

### **List of Figures and Tables**

Figure 1. Scanning electron micrograph of a vascular bundle...	pg. 6
Figure 2. Scanning electron micrograph of a cross-section of bamboo...	pg. 7
Figure 3. Schematic of indentation locations in a typical bamboo sample.	pg. 12
Figure 4. Nanoindentation locations in a bamboo sample.	pg. 19
Figure 5. An overlay of several cross-sectional SEM micrographs of bamboo.	pg. 20
Figure 6. An overlay of two longitudinal SEM micrographs of bamboo.	pg. 20
Figure 7. Scanning electron micrograph of a vascular bundle for cell analysis.	pg. 21
Figure 8. Histogram of sclerenchyma cell sizes found in Figure 7	pg. 22
Figure 9. Scanning electron micrograph of parenchyma cells	pg. 23
Figure 10. Histogram of parenchyma cell sizes found in Figure 9	pg. 23
Figure 11. Histograms of sclerenchyma cell sizes as a function of radial position	pg. 24
Figure 12. Area fraction of solid material in parenchyma and sclerenchyma	pg. 25
Figure 13. Stress-strain curves for bamboo samples in compression	pg. 28
Figure 14. Failure of bamboo during a compressive loading test.	pg. 29
Figure 15. Images of a bamboo specimen which failed during compression.	pg. 29
Figure 16. Image of a bamboo specimen which failed during compression.	pg. 30
Figure 17. Compressive strength versus density plots for bamboo samples.	pg. 30
Figure 18. Compressive strength versus density plots for bamboo samples.	pg. 31

### **List of Tables**

Table 1. Young's elastic modulus and hardness of sclerenchyma fibers.	pg. 18
Table 2. Various dimensions of both sclerenchyma and parenchyma cells	pg. 23
Table 3. Compressive strength, density, and Young's modulus of bamboo	pg. 27

## **1. Introduction**

Bamboo has phenomenal potential as a construction material, and holds many advantages over more traditional materials such as wood, steel, and concrete. For example, bamboo grows much more rapidly than wood and can be harvested in as little as five years [1]. Using bamboo provides an environmental advantage over steel and concrete, as the production of steel and concrete is more energy intensive and generates more pollution [2]. Furthermore, bamboo is readily available in rapidly growing nations such as India and China [3].

One approach to using bamboo as a structural material in construction is to create a glue-laminated composite bamboo material similar to plywood or oriented strandboard. These materials are commonly known as *structural bamboo products* and have been used in several test structures throughout China, including a bridge for motor vehicles [3] and a modern house [4].

A significant limitation to the widespread usage of structural bamboo products is the lack of building safety codes for these materials. This thesis work is part of a larger project aimed at characterizing the mechanical properties of bamboo and using that information to produce a model to predict the properties of structural bamboo products.

### **1.1 Microstructure of bamboo**

Bamboo is primarily composed of two types of cells. Stiff, fibrous sclerenchyma cells run along the length of the bamboo, providing much of the structural support. These sclerenchyma cells surround two or three channels, which are used for transport of water and nutrients. These sclerenchyma cells and channels are organized into discrete collections called vascular bundles. Surrounding the vascular bundles is a matrix of soft, less dense parenchyma

cells [5]. Unlike the sclerenchyma, these cells are polyhedral and behave like a foam. The two different types of cells can be seen in Figure 1.

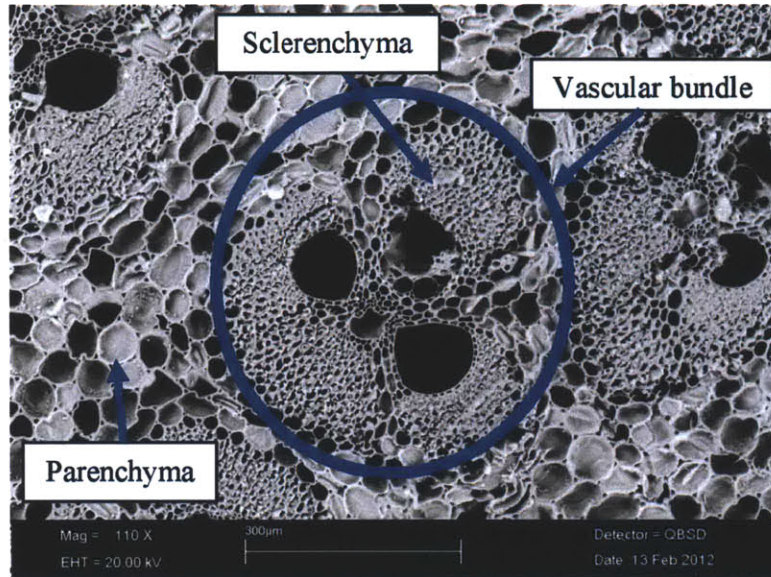


**Fig. 1.** Scanning electron micrograph of a vascular bundle of sclerenchyma cells surrounded by the parenchyma matrix.

The density of vascular bundles increases from the inner edge to the outer edge of the bamboo, as can be seen in Figure 2. This variation in microstructure causes many of bamboo's mechanical properties to have a gradient from the inner edge to the outer edge. For instance, the density, tensile strength, and tensile Young's modulus is found to increase towards the outer edge of many bamboo species [6].

In this thesis, the variation in bamboo microstructure will be investigated with a scanning electron microscope. This microstructural information will be compared with macroscopic compressive loading experiments and nanoindentation experiments to model the mechanical properties of bamboo.



**Fig. 2.** Scanning electron micrograph of a cross-section of bamboo, showing the variations in microstructure from the inner to the outer edge.

### 1.2 Modeling of bamboo as a cellular solid

A *cellular solid* is “an assembly of cells with solid edges or faces, packed together so that they fill space” [7]. The long, prismatic sclerenchyma cells in bamboo can be modeled as a honeycomb-like cellular solid loaded out-of-plane, while the polyhedral parenchyma cells can be modeled as a closed-cell foam.

A honeycomb-like cellular solid is defined as having prismatic cells whose cross-sections can tile to fill a plane [7]. The mechanical properties of a honeycomb-like cellular solid are therefore dependent upon direction: applying stress in the plane of the solid (the plane shown in Figures 1 and 2) causes the cell walls to bend as the cross-section of the cell deforms, while applying stress out-of-plane (into and out of the page in Figures 1 and 2) causes the cell walls to stretch or compress, rather than bending. The compression tests performed in this work correspond to out-of-plane compressive loading of the sclerenchyma. The out-of-plane Young’s

modulus of a honeycomb-like cellular solid  $E_3^*$  is equal to the Young's modulus of the solid cell wall material  $E_s$  multiplied by the relative density of the cellular solid ( $\rho^*/\rho_s$ ):

$$E_3^* = E_s \frac{\rho^*}{\rho_s}$$

The relative density of the cellular solid is simply the density of the cellular solid divided by the density of the solid cell wall material. The relative density is equivalent to the volume fraction of solid material in the cellular solid, which is approximated in this work by analyzing scanning electron micrographs.

Honeycomb-like cellular solids can fail by plastic yielding or brittle fracture of the cell walls once a critical stress has been reached. This critical stress can be calculated from the bulk solid properties based on the mechanism of deformation or failure. For honeycombs loaded out-of-plane, the critical stresses for yielding ( $\sigma_y^*$ ) and fracture ( $\sigma_f^*$ ) both depend on the relative density and either the yield stress  $\sigma_{ys}$  or fracture stress  $\sigma_{fs}$  of the solid [7]:

$$\sigma_y^* = \sigma_{ys} \frac{\rho^*}{\rho_s}$$

$$\sigma_f^* \approx 12\sigma_{f,3} \frac{\rho^*}{\rho_s}$$

Both of these equations are considered upper bounds on the compressive strength of the honeycomb loaded out-of-plane. Therefore, experiments measuring the mechanical properties of honeycomb-like cellular solids like bamboo are of critical importance in further understanding how these solids fail under loading.



Unlike the sclerenchyma fibers, the parenchyma cells are not long and prismatic, and therefore the modeling described above is not well suited for describing the mechanical properties of parenchyma. Parenchyma cells are better approximated as a closed-cell foam, in which polyhedral cells with closed faces stack together to fill space. The mechanical properties of closed-cell foams depend not only on the relative density of the foam but also the amount of the solid cell wall material located at a cell edge versus a cell face, as the mechanical properties of closed-cell foams are dominated by stretching of the cell faces. Furthermore, if the foam contains a fluid, the fluid can become pressurized as the cells deform, which influences the mechanical properties [7]. In this thesis, all experiments were performed with dry bamboo to avoid significantly altering the mechanical properties of the parenchyma. Ignoring the possibility of pressurizing a fluid inside the cells, the Young's modulus of a closed-cell foam with a fraction of solid in cell faces of  $\varphi$  goes as [7]:

$$\frac{E^*}{E_s} \approx \varphi^2 \left( \frac{\rho^*}{\rho_s} \right)^2 + (1 - \varphi) \left( \frac{\rho^*}{\rho_s} \right)$$

As a closed-cell foam is loaded, it will deform in a linear elastic manner until it reaches a critical stress and begins to collapse, either elastically, plastically, or by crushing of the cell walls. The elastic buckling criterion is related to the Young's modulus of the solid material and its relative density [7]:

$$\frac{\sigma_{el}^*}{E_s} \approx 0.03 \left( \frac{\rho^*}{\rho_s} \right)^2 \left( 1 + \left( \frac{\rho^*}{\rho_s} \right)^{1/2} \right)^2$$

The maximum stresses for plastic yielding and brittle crushing of closed-cell foams follow similar scaling laws to each other based on the relative density of the solid:

$$\frac{\sigma_y^*}{\sigma_{ys}} \approx \left( \varphi \frac{\rho^*}{\rho_s} \right)^{3/2} + (1 - \varphi) \left( \frac{\rho^*}{\rho_s} \right)$$

$$\frac{\sigma_f^*}{\sigma_{fs}} \approx \left( \varphi \frac{\rho^*}{\rho_s} \right)^{3/2} + (1 - \varphi) \left( \frac{\rho^*}{\rho_s} \right)$$

Ultimately, comparing the mechanical properties of bulk bamboo samples to their densities should reveal a correlation which will determine which of the above discussed mechanisms is dominant in the failure of bamboo.

However, for the models described above to accurately reflect the mechanical properties of bamboo, it must be assumed that the properties of the solid cell wall material do not depend on relative density. In some species of palm trees, which have similar microstructures to bamboo, the Young's modulus of the solid material does depend on the relative density, causing a nonlinear dependence of the Young's modulus of the bulk material on the relative density [8]. To confirm whether or not the properties of the solid sclerenchyma fiber material changes with relative density, nanoindentation experiments will be carried out on fibers located in various locations in the stalk. Because the volume fraction of solid in the vascular bundles changes with radial position in the stalk, any variation in mechanical properties at different locations could provide evidence of a dependence of the mechanical properties of the cell wall material on relative density.

## **2. Methods and Materials**

Stalks of *Phyllostachis dulcis* bamboo were obtained from the Arnold Arboretum at Harvard University. From these stalks, bamboo samples were cut for one of three purposes: nanoindentation, scanning electron microscopy, or mechanical testing. The sample preparation and testing procedure for each test is outlined in the following three sections.

### **2.1. Nanoindentation**

To prepare the bamboo for nanoindentation, bamboo stalks were cross-sectioned at different heights and mounted in Struers Epofix resin (Struers, Copenhagen, Denmark). The three cross-sections chosen randomly for this study are labeled 1.3, 2.15A, and 2.18C. These labels identify from which bamboo stalk the cross-section came, as well as the approximate location of the cross-section taken from the stalk. Sample 1.3 came from one stalk of *Phyllostachis dulcis*, between 19 and 27 inches (48 and 69 cm) up from the bottom of the stalk. Samples 2.15A and 2.18C both came from a second stalk, but from different heights along this stalk. Sample 2.15A was cut from between 146 and 155 inches (371 and 393 cm) up from the bottom of the stalk, while sample 2.18C was cut from higher up the stalk, between 163 and 170 inches (414 and 432 cm).

The top surface of each cross-section was ground and polished to a flat surface by hand using a Struers Rotopol-1 model polishing wheel and varying grades of Struers waterproof silicon carbide sandpaper. Starting with a 600-grit sandpaper wheel, the cross-sectioned surface was polished and inspected via optical microscope until all grooves larger than the sandpaper particle size had been removed. This process was repeated with 1200, 2000, and 4000 grit sandpaper. The polished surface was then covered in a layer of Parafilm wax paper to protect it,

and the backside was ground using coarse sandpaper until the back surface was parallel to the polished surface. The Parafilm coating was removed before nanoindentation.

When polishing was completed, the samples were glued to magnetic stainless steel substrates using Loctite 454 Prism superglue (Henkel AG & Co., Düsseldorf, Germany). Clusters of indentations were performed at eight locations on each bamboo cross section, with an “inner” and “outer” location in each of four quadrants, labeled “North”, “South”, “East”, and “West”. Each location was chosen to lie within a region of sclerenchyma fibers. A schematic of indentation locations is shown in Figure 3.

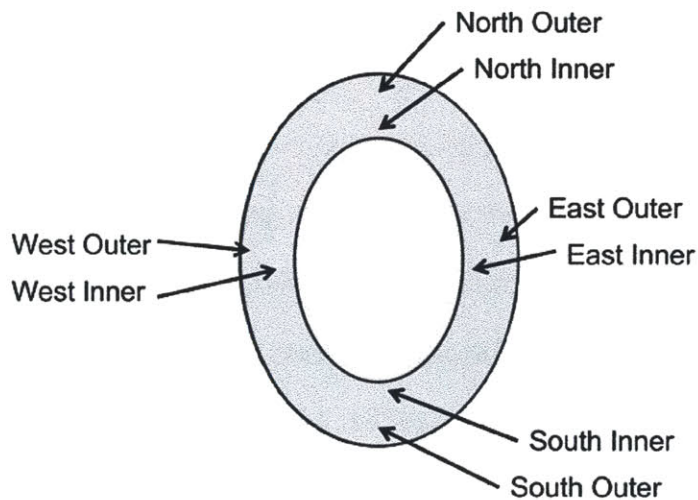


**Fig. 3.** Schematic of indentation locations in a typical bamboo sample.

In each location, a five-by-five grid of 25 indentations was performed, using a Hysitron triboindenter, using a 200nm radius Berkovich tip (Hysitron, Minneapolis, MN). The indentations were spaced 15  $\mu\text{m}$  apart. Upon making contact with the sample surface, the load was increased by 50  $\mu\text{N/s}$  to 500  $\mu\text{N}$ , held at 500  $\mu\text{N}$  for 5 seconds, and then decreased by 50  $\mu\text{N/s}$  until it returned to zero.

Oliver-Pharr analysis [10] was used on the unloading section of each load-displacement curve to determine the hardness and Young's modulus at each indentation point. The hardness and Young's modulus at each point were averaged for each of the eight indentation clusters, and results are reported in Section 3.1, Table 1.

## 2.2 Scanning electron microscopy

To investigate the microstructure of the bamboo specimens, a LEO VP438 scanning electron microscope (SEM) was used to take micrographs at various magnifications. To prepare bamboo samples for imaging, a thin cross-section approximately 5mm thick was cut from the stalk and allowed to soak in water for at least four hours. The cross-section was then further sectioned by slicing in the radial direction with a sterile surgical blade (Feather Industries Limited, Tokyo, Japan). Finally, a cut was made with a new sterile blade, parallel to the original cross section surface, to prepare that surface for imaging. The samples were allowed to dry for at least 24 hours before imaging.

The scanning electron microscope was operated in variable pressure mode with a chamber pressure of approximately 20 Pa to avoid charging the non-conductive bamboo samples during imaging. Micrographs were taken at various magnifications of the cross-sectional surface of the bamboo samples using the backscatter detector. A series of overlapping images was taken which panned across the bamboo sample from the outer edge to the inner edge, and these images were later overlaid using Adobe Photoshop software (Adobe Systems Incorporated, San Jose, CA) to produce a map of the microstructure in the radial direction. The sample was then tilted 90 degrees using the microscope's movable stage to obtain micrographs of the bamboo microstructure in the longitudinal direction.

### 2.3 Microstructure analysis

The image analysis software ImageJ (National Institutes of Health, Bethesda, MD) was used to identify and characterize fiber bundles and parenchyma cells in the SEM micrographs [9]. The scale of the images was set by selecting the scale bar included on each micrograph and using the “Analyze – Set Scale” function. Cell wall measurements were then made using the software’s ruler tool.

Using the “Image – Adjust – Threshold” function, images were converted from grayscale to black and white based on the brightness of each pixel. Any pixel below a threshold brightness value was converted to a black pixel, and all other pixels were converted to white. The threshold brightness value was determined by visually inspecting a preview of the resulting image to ensure that the desired cell type could be easily identified. Once the grayscale image was converted to a strictly black and white image, the “Analyze – Analyze Particles” function was used to quickly count and characterize the desired cells. The Analyze Particles function measures and reports the area of the void within each cell, which can be used to calculate the area fraction of cell wall material and of void in each image.

To simultaneously measure the area fractions of parenchyma cells, sclerenchyma cells, and the void area fraction as a function of radial position, a map of the microstructure of a bamboo sample was made by overlaying several SEM micrographs using Adobe Photoshop software. The image was cropped at varying radii, and sclerenchyma fibers in each cropped image were counted and their areas measured using the ImageJ software.

### 2.4 Mechanical testing

To measure the compressive strength and Young’s modulus of bamboo, short cylinders ranging from 10 to 30 mm in height were machined to various thicknesses using several tools.

First, cuts were made perpendicular to the stalk using either a hacksaw or a lathe. The lathe was operated at 700 rpm and the lathe tool was slowly moved inward by hand, gradually shaving away bamboo until the tool had cut all the way through. The lathe must be operating at a high spin speed and low feed rate to avoid tearing fibers out of the bamboo.

After several cylinders of the same height had been cut from the stalk, each cylinder was machined with a Dremel Multi-Pro Model 395 rotary tool (Robert Bosch GmbH, Gerlingen, Germany) operating at 15-20,000 rpm, or between speed settings 5 and 6. Bamboo material was removed from the outside in, to produce cylindrical shells of varying thicknesses. The samples were then polished on a Struers Rotopol-1 polishing wheel using 500-grit sandpaper to ensure that both faces of the sample were parallel to each other. The major and minor inner and outer diameters and the height were measured with calipers to estimate the volume of the bamboo, by approximating it as a prism with an elliptical cross-section and using the following equation:

$$V = \frac{h * \pi(OD_1 * OD_2 - ID_1 * ID_2)}{4}$$

where  $h$  corresponds to the height of the sample,  $OD_1$  and  $OD_2$  are the major and minor outer diameters of the sample, respectively, and  $ID_1$  and  $ID_2$  are the major and minor inner diameters of the sample. The mass of each sample was measured using a Cole-Parmer Symmetry ECII balance (Cole-Parmer, Vernon Hills, IL).

Following these measurements, the samples were compressed in an Instron 1321 frame controlled by a model 8500 Plus controller (Instron, Norwood, MA) at a rate of 1 mm/min for either 2 or 3 minutes. The load was measured using the Instron's load cell, while the displacement was measured using a direct-current linear variable differential transformer

(LVDT) made by Trans-Tek, Inc. (model 0243-0000, Ellington, CT), connected to a DC power supply (Hewlett-Packard model E3612A, Palo Alto, CA) outputting at 15 V. The load and displacement were recorded using a National Instruments data acquisition module (NI USB-6211) and LabView software (National Instruments, Austin, TX).



### **3. Results and discussion**

#### **3.1 Nanoindentation**

Young's elastic modulus and hardness of the sclerenchyma fibers are reported for the three bamboo samples in Table 1. Neither the Young's modulus nor the hardness of these fibers appears to change significantly with radial position (inner/outer) or with the quadrant in which the indentation occurred (north, south, east, or west). The Young's modulus values found for sample 2.15A tended to be slightly greater than those found for sample 2.18C, which was cut from a higher location on the same stalk. While sample 1.3 was cut from a lower position, it was also cut from a different stalk, and therefore may be of a different age, which can change the stiffness of the fibers [1]. Confirming that the mechanical properties of the sclerenchyma fiber do not vary with position simplifies modeling of bamboo, as the properties of the solid can be assumed to be constant rather than dependent upon composition.

In general, the Young's modulus of the fibers ranged from 15 to 17 GPa, while hardness ranged from 360 to 530 MPa. These values are in agreement with Yu's group, who also performed nanoindentation experiments on Moso bamboo (*Phyllostachys edulis*) [11]. However, other methods of calculating the Young's modulus of the fibers show that nanoindentation may be significantly underestimating this property. For instance, Nogata *et al.* estimate the Young's modulus of bamboo sclerenchyma fibers to be 55 GPa by measuring the Young's modulus of macro scale bamboo samples, calculating the volume fraction of fibers, and extrapolating their results to 100% fiber [6]. Rao and Rao were able to mechanically extract Moso bamboo fiber and performed tensile loading tests to measure the Young's modulus, reporting a value of 35.91 GPa [12]. Yu suggests that the fibers are significantly less stiff perpendicular to the longitudinal

direction of the fiber, and that nanoindentation measurements represent a mixture of the Young's modulus in all directions [11].

Location		Sample 1.3		Sample 2.15A		Sample 2.18C	
		Young's Modulus (GPa)	Hardness (MPa)	Young's Modulus (GPa)	Hardness (MPa)	Young's Modulus (GPa)	Hardness (MPa)
North	Inner	16.3 ± 2.1	420 ± 70	16.8 ± 1.0	460 ± 40	14.5 ± 2.7	360 ± 90
	Outer	16.6 ± 1.9	440 ± 60	17.2 ± 1.6	460 ± 60	16.3 ± 2.0	440 ± 90
South	Inner	16.9 ± 1.6	390 ± 130	16.4 ± 1.4	420 ± 40	15.2 ± 1.9	390 ± 90
	Outer	14.8 ± 3.0	400 ± 90	17.2 ± 1.1	470 ± 40	15.4 ± 1.7	400 ± 70
East	Inner	15.4 ± 0.9	430 ± 40	16.7 ± 1.2	440 ± 50	15.6 ± 1.3	390 ± 60
	Outer	15.3 ± 1.1	410 ± 50	17.7 ± 1.0	530 ± 50	15.3 ± 1.4	410 ± 50
West	Inner	15.7 ± 1.9	400 ± 60	16.2 ± 0.8	420 ± 40	15.9 ± 1.2	450 ± 70
	Outer	15.0 ± 1.2	380 ± 50	17.4 ± 1.2	480 ± 70	16.0 ± 1.8	400 ± 80

**Table 1.** Young's elastic modulus and hardness of sclerenchyma fibers at various positions in each of three cross-sectioned bamboo samples.

As can be seen in Figure 2, the bundles of sclerenchyma fibers appeared to become smaller towards the center of the bamboo stalks, or the "inner" positions. In one case, the indentation grid did not fit on the fiber bundle, causing one column of indentations in the grid to show significantly lower values of Young's modulus and hardness (2.15A E inner). These values were not used to calculate the fiber Young's modulus reported in Table 1. The calculated Young's moduli for these five indentations varied from 1.9 to 11.7 GPa, while the hardness varied from 20 MPa to 830 MPa. The large spread in these values may indicate that some indentations were taken on the border between the stiffer sclerenchyma cells and the soft, porous parenchyma cells, resulting in a mixture of measured moduli. Yu *et al.* report that the Young's

modulus of parenchyma cell walls is 5.8 GPa, and the hardness 230 MPa, as determined by nanoindentation, which agrees with the range of values found above [11].

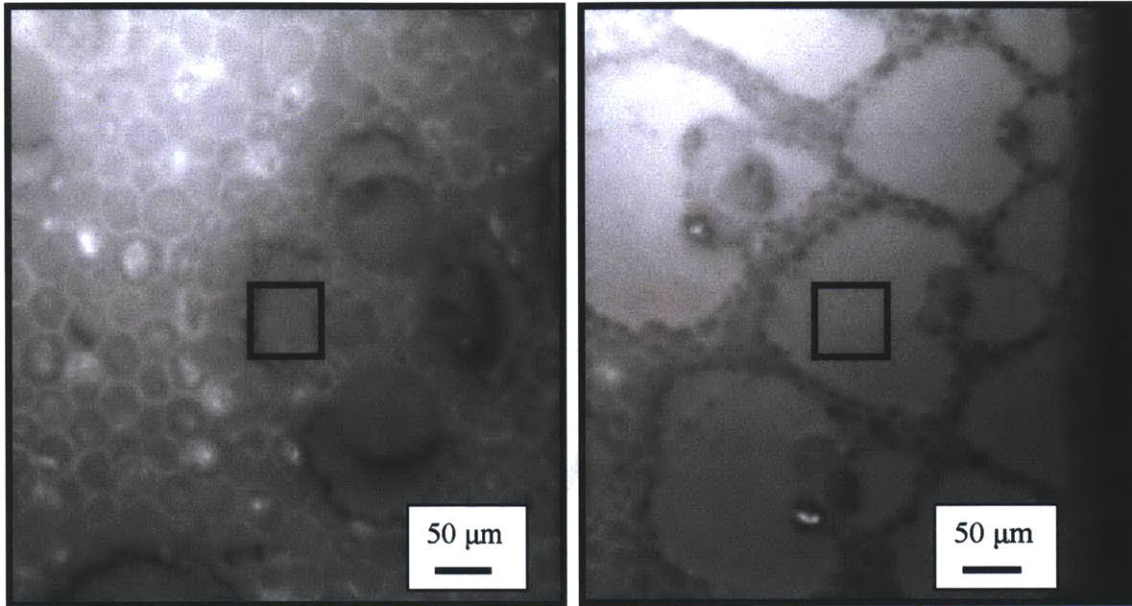


**Fig. 4.** East inner (left) and east outer (right) locations for indentations in Sample 2.15A. The black square represents an approximate area of indentation.

### 3.2. SEM micrographs and microstructure analysis

SEM micrographs perpendicular to the direction of growth confirm the well-known microstructure of bamboo. The bamboo samples are composed of bundles of sclerenchyma fibers, which run along the length of the bamboo stalk, and a matrix of polyhedral parenchyma cells. The density of sclerenchyma fibers increases towards the outside of the bamboo and decreases toward the inside of the bamboo, as can be seen in Figure 5 below.

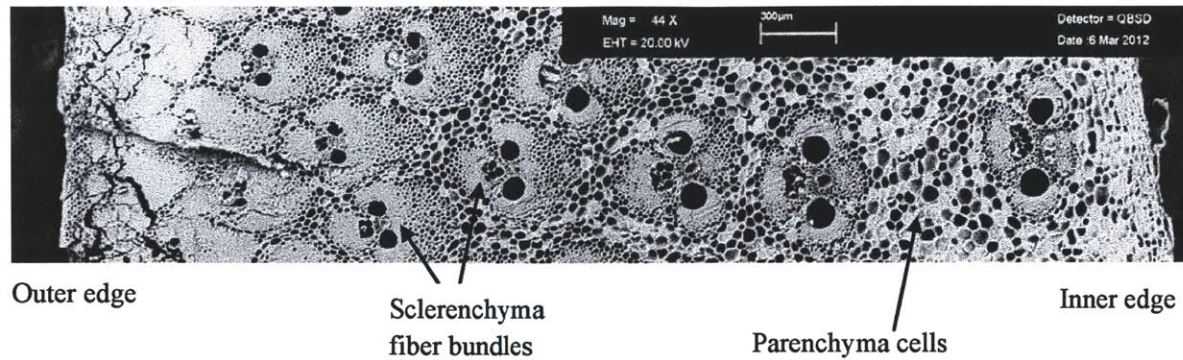


**Fig. 5.** An overlay of several scanning electron micrographs showing the variation in microstructure from the outer to the inner edge of the bamboo specimen.

SEM micrographs were also taken perpendicular to the face shown in Figure 5. These images show that the sclerenchyma cells are prismatic and continue down the length of the bamboo stalk, while the parenchyma cells are polyhedral. An example micrograph in the longitudinal direction is shown in Figure 6 below.

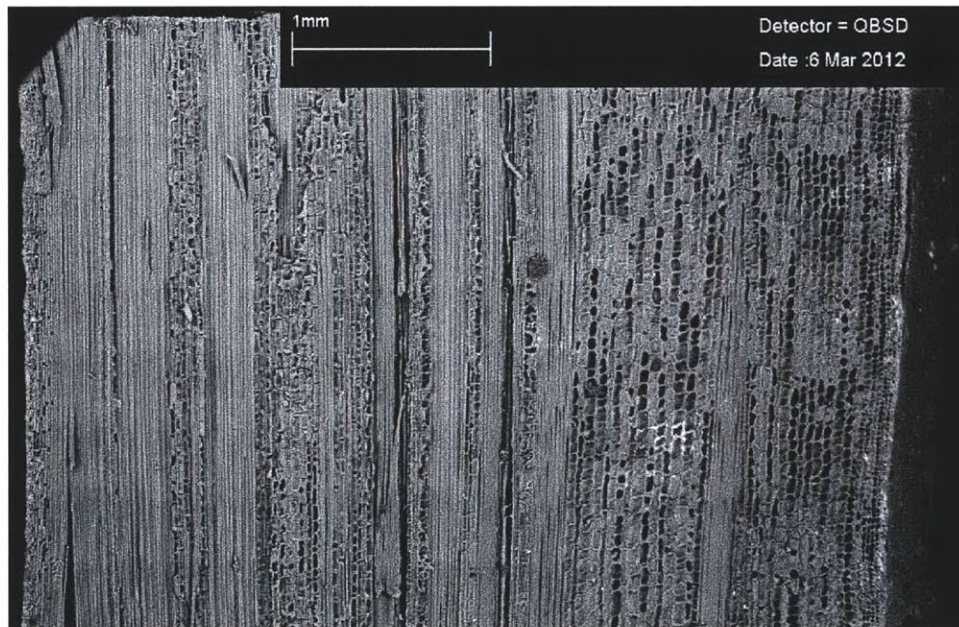


**Fig. 6.** An overlay of two scanning electron micrographs showing the long, prismatic sclerenchyma cells and polyhedral parenchyma cells.

Some images were selected for analysis of the size and porosity of sclerenchyma fibers and parenchyma cells using NIH's ImageJ software. Figure 7 shows an SEM micrograph which yielded interesting data on sclerenchyma cells.

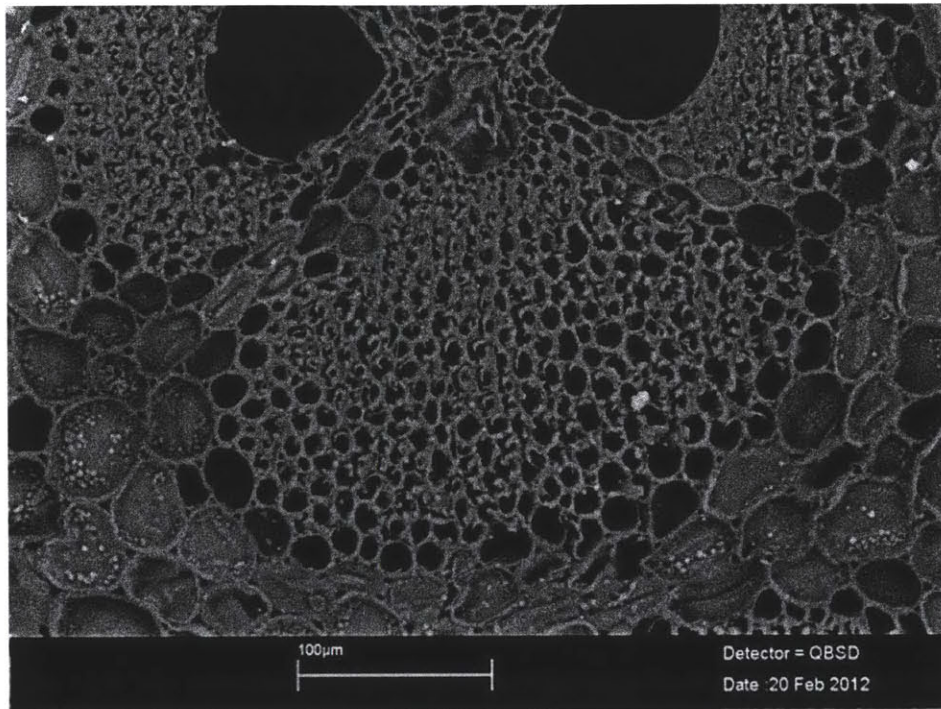


**Fig. 7.** SEM micrograph of a bamboo sample taken from a height of approximately 50 cm from the ground. This vascular bundle was located approximately 2mm away from inner edge.

The ruler function of the ImageJ software was used to measure twenty sclerenchyma cell wall widths, and the average cell wall width was found to be  $1.9 \pm 0.5 \mu\text{m}$ . The cross-sectional areas of the sclerenchyma cells were also measured using the Analyze Particles function of the ImageJ software, yielding a wide distribution of areas ranging from 10 to  $200 \mu\text{m}^2$ , with an average of  $52 \pm 40 \mu\text{m}^2$ . A histogram of cell areas in Figure 7 shows the distribution of cell sizes. By comparing the area of void within the cells to the area of the entire fiber bundle, an estimate of the volume fraction of solid material in the fiber bundle can be made. The volume fraction of solid material in this fiber bundle was found to be approximately  $0.6 \pm 0.05$ . These

results are summarized in Table 2. However, as can be seen in Figure 2, the volume fraction of solid material in the sclerenchyma fiber bundles is affected by radial position and approaches 1 near the outer edge of the bamboo specimen.

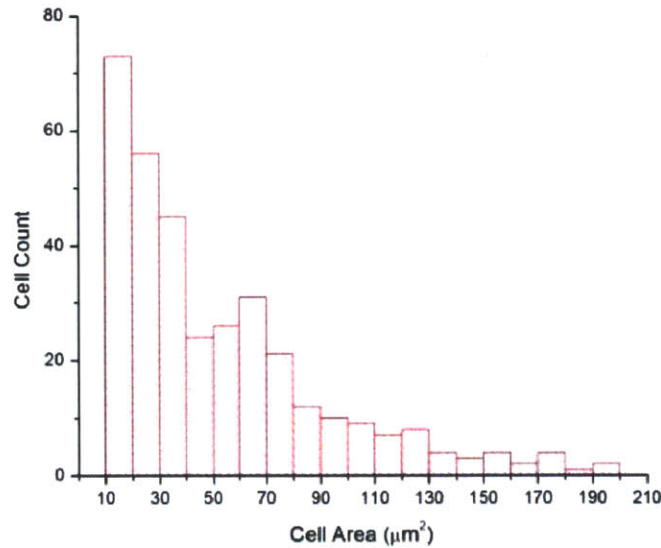


**Fig. 8.** Histogram of sclerenchyma cell sizes of the vascular bundle in Figure 7.

A similar analysis can be performed on micrographs of parenchyma cells. In Figure 9 below, the parenchyma cells on the left and right side of the picture were analyzed. The average cell wall width was found to be  $2.4 \pm 0.7 \mu\text{m}$ , and again a wide distribution of cross-sectional areas was found for the cells. The average cross-sectional area for parenchyma cells was found to be  $1400 \pm 1100 \mu\text{m}^2$ , much larger than that for sclerenchyma cells. Because the cells are larger, the volume fraction of solid material in the parenchyma matrix is much smaller than in the sclerenchyma fibers. The volume fraction of solid material in the parenchyma matrix was found to be approximately  $0.15 \pm 0.04$ , estimating by tracing the cell walls of ten cells and measuring their areas. Due to issues with image contrast and brightness, this is an overestimate

of the volume fraction of solid, as bright pixels near the edge of a parenchyma cell count as a cell wall when in fact they may not lie in the plane of the cross-section.

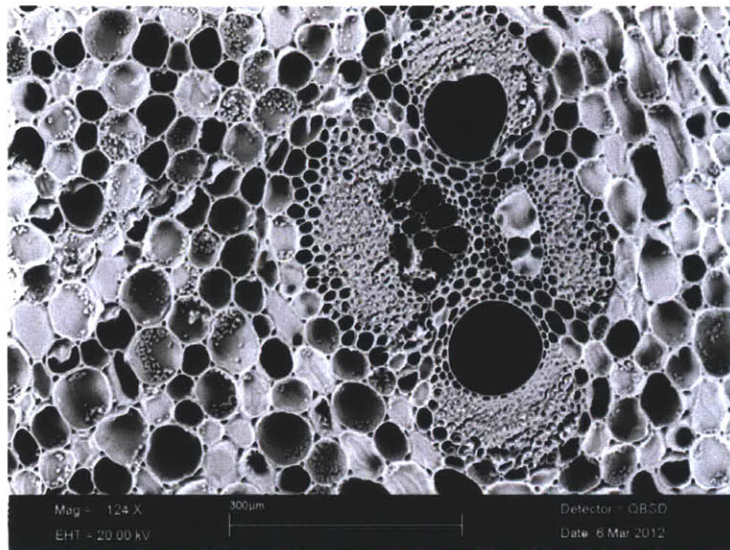


**Fig 9.** SEM micrograph of a sample taken 15 cm up from the bottom of the stalk. This image was taken approximately 0.5 mm from inner edge.

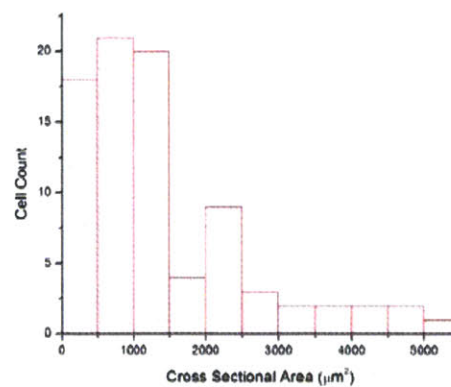
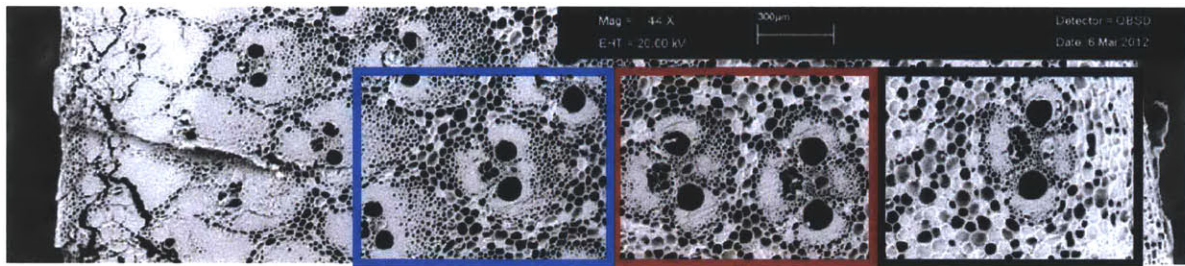


**Fig. 10.** Histogram of parenchyma cell areas in Figure 9.

**Table 2.** Various dimensions of both sclerenchyma and parenchyma cells as determined by SEM image analysis.

Cell Type	Cell Wall Width (µm)	Cell Cross-Sectional Area (µm <sup>2</sup> )	Volume Fraction of Solid Material
<b>Sclerenchyma</b>	1.9 ± 0.5	52 ± 40	0.6 ± 0.05
<b>Parenchyma</b>	2.4 ± 0.7	1400 ± 1100	0.15 ± 0.05



Outer edge

Inner edge

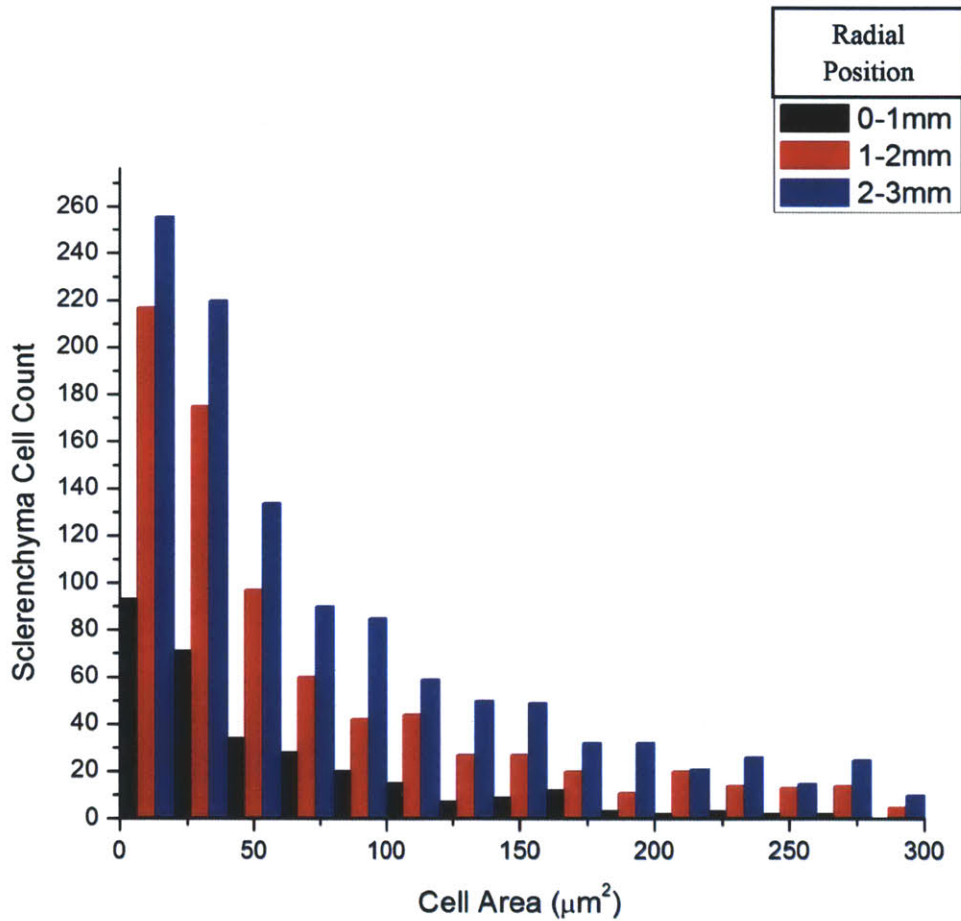


**Fig. 11.** Size distributions of sclerenchyma cells within three 1-mm wide boxes extending radially outward from the inside edge of the stalk.

The size distribution of sclerenchyma cells in vascular bundles was also measured as a function of radial position in the stalk. As can be seen in Figure 11, three 1-mm wide regions were selected, spanning from the inner edge of the bamboo specimen outwards, and histograms



representing the size distribution of sclerenchyma cells are plotted on the same set of axes. Because there are more vascular bundles towards the outer edge of the bamboo specimen, the number of cells of each size increases towards the outer edge as well. However, the relative distributions have roughly the same general shape regardless of radial position, indicating that the vascular bundles themselves do not vary much with respect to radial position.

The micrograph shown in Figure 11 was divided into four 1 mm wide rectangular regions, and the area fractions of solid material in both sclerenchyma and parenchyma cells was measured for each box. From these values, the total area fraction of solid material for both cells was calculated. All three of these values are plotted as a function of radial position in Figure 12 below. In this case, radial position is defined as the distance  $r$  between the outer edge of the box and the inner edge of the bamboo sample, divided by the distance  $r_0$  between the inner and outer edges of the sample.

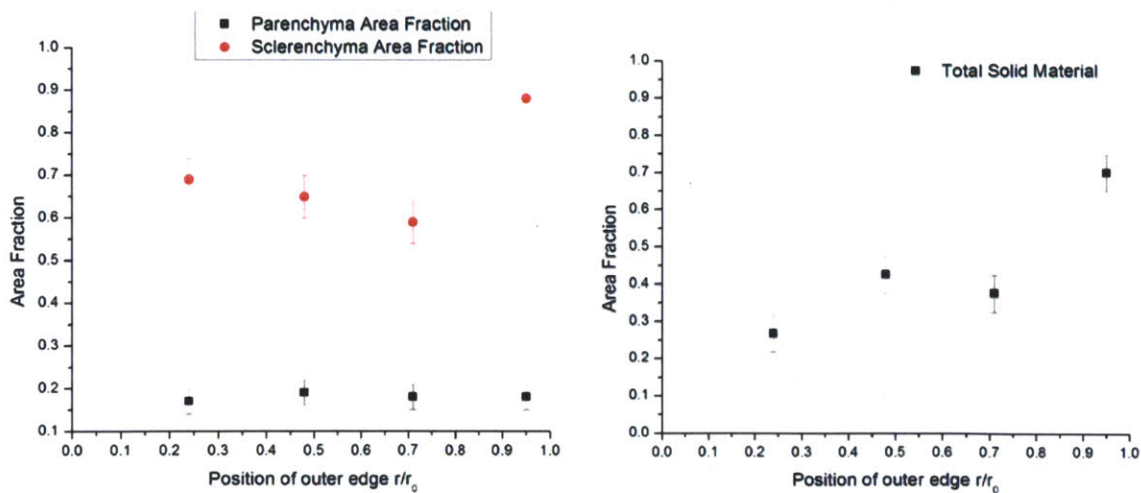


**Fig. 12.** (a) Area fraction of solid material in parenchyma and sclerenchyma cells and (b) total area fraction of solid material as a function of radial position.

The area fraction of solid material in the parenchyma cells stays roughly constant with respect to position at approximately  $0.18 \pm 0.03$ . However, due to the brightness and resolution of the SEM micrograph, this is expected to be an overestimate of the actual value. In contrast, the area fraction of solid material in the sclerenchyma fibers does seem to change from the inner radius to the outer, staying roughly constant until reaching the outer quarter of the sample, where the area fraction of solid begins to increase, indicating that the sclerenchyma fibers are becoming denser towards the outside. One consideration to keep in mind is that the set of micrographs may have produced too narrow an image to be representative of the entire bamboo specimen, which could explain why the area fraction of solid does not seem to change continuously.

### 3.3. Mechanical testing

To examine how bamboo's microstructure influences its mechanical properties, cylindrical samples of bamboo were prepared with various thicknesses to highlight mechanical differences between the inner and outer portions of the bamboo stalk. Eight samples were prepared from two different locations in the stem: samples 1-4 were cut from a segment between 11 and 17 cm from the bottom of the stalk, and samples 5-8 were cut from a segment between 110 and 120 cm from the bottom of the stalk. Samples 4 and 8 correspond to full cross-sections of bamboo. Stress-strain curves for each sample are shown in Figure 13.

The discrepancy in Young's moduli between the two sets of samples can be attributed to differences in sample preparation. Samples 1-4 were not machined by lathe and polished to ensure flat, parallel surfaces, but instead were cut by hand with a hacksaw. These samples ranged from 5.25mm to 5.54mm in height. Assuming a yield strain in the bamboo sample as high as 10% means that if one portion of the bamboo surface sits just 0.5 mm above another portion of the surface, some parts of the bamboo will have yielded before other parts have been

loaded. This results in inaccurate measurements of Young's modulus in compression. To counteract this effect, extra care was taken in preparing the second set of samples. The samples were made longer and were machined by lathe, and the ends were polished. The compressive Young's modulus of an entire cross-section, measured to be  $7.2 \pm 0.2$  GPa, is roughly a factor of two lower than reported values in the literature for Young's modulus in tension of 15 GPa [6].

**Table 3.** Mechanical properties of bamboo as a function of radial thickness. Radial position  $t/t_0$  is a ratio of the thickness of the sample to the thickness of the stalk from which it was cut. The values of Young's modulus are extremely unlikely compared to literature values, and this discrepancy is likely due to poor sample preparation as described below.

Sample	Radial Thickness (mm)	Radial Position $t/t_0$	Density ( $\text{kg/m}^3$ )	Compressive Strength (MPa)	Young's Modulus (GPa)
1	$1.0 \pm 0.1$	$0.25 \pm 0.05$	$520 \pm 30$	$40 \pm 4$	$0.56 \pm 0.03$
2	$2.0 \pm 0.1$	$0.50 \pm 0.05$	$480 \pm 20$	$47 \pm 5$	$0.61 \pm 0.03$
3	$2.5 \pm 0.2$	$0.63 \pm 0.08$	$560 \pm 30$	$63 \pm 6$	$0.51 \pm 0.03$
4	$4.0 \pm 0.2$	1	$610 \pm 30$	$86 \pm 9$	$0.3 \pm 0.02$
5	$1.0 \pm 0.2$	$0.4 \pm 0.1$	$670 \pm 30$	$46 \pm 5$	$4.7 \pm 0.2$
6	$1.5 \pm 0.1$	$0.60 \pm 0.08$	$700 \pm 35$	$60 \pm 6$	$5.4 \pm 0.2$
7	$2.0 \pm 0.1$	$0.8 \pm 0.1$	$760 \pm 35$	$76 \pm 8$	$5.8 \pm 0.2$
8	$2.5 \pm 0.2$	1	$800 \pm 40$	$96 \pm 9$	$7.2 \pm 0.2$

The measured densities also varied significantly between the two sets of samples. While the density could change with height, a more likely explanation is that the moisture content of the samples was not carefully controlled. Extra moisture present in the second set of samples could add extra weight and cause an overestimate of the density.

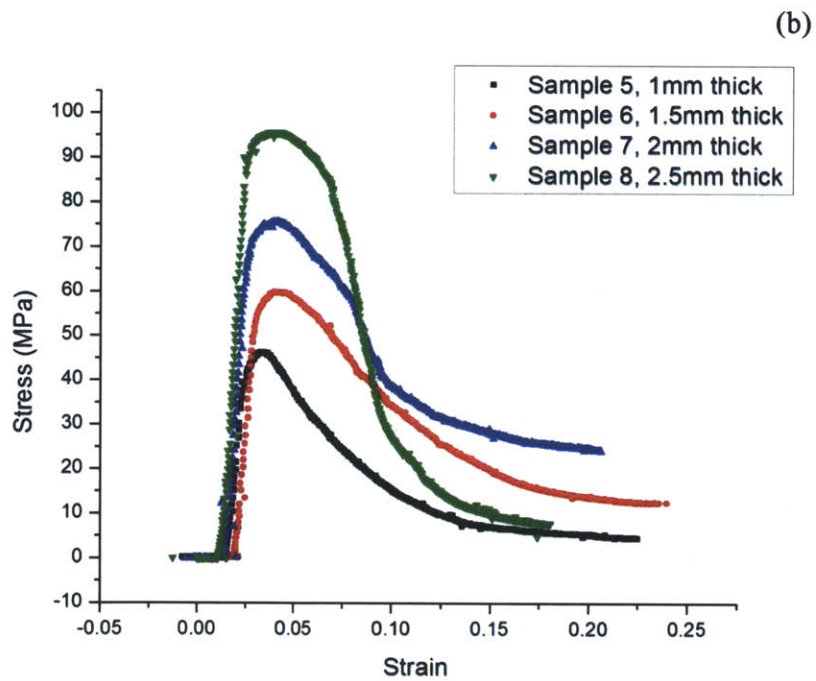
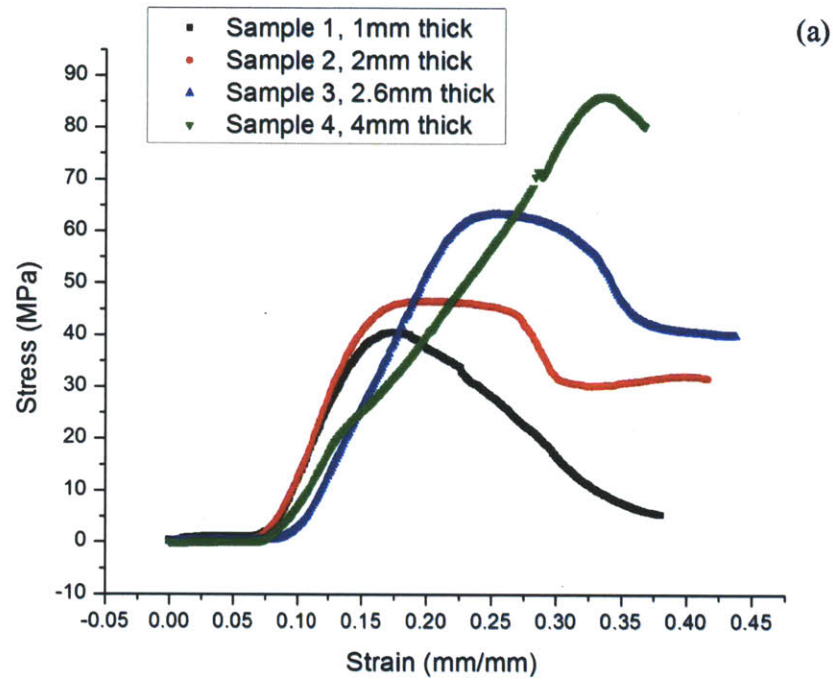


**Fig. 13.** Stress-strain curves for (a) samples 1-4, taken from approximately 15 cm up the stalk, and (b) samples 5-8, taken from approximately 115 cm up the stalk.

The failure of the bamboo samples was consistent among all samples. The bamboo rings would tend to fail by splitting longitudinally into columns and buckling along those columns. Images of the failure of bamboo are shown in Figures 14-16. In some cases, as shown in Figure 16, cracks would form around the circumference as well as in the radial direction.

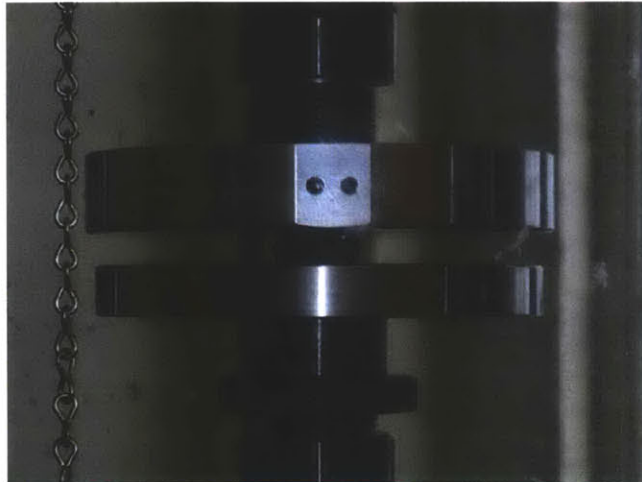


**Figure 14.** Failure of bamboo during a compressive loading test.

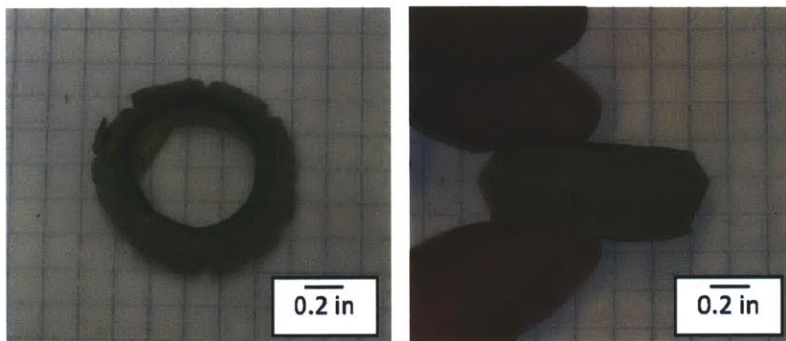


**Figure 15.** Cross-sectional (a) and longitudinal (b) images of a bamboo sample that failed during compressive loading.

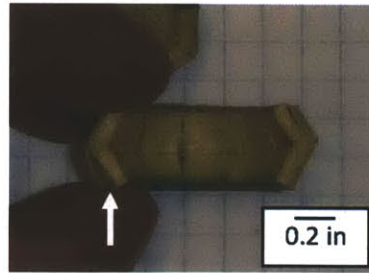


**Figure 16.** After compressive loading, a sample fell apart during handling, revealing a cross-section in the longitudinal direction. The bamboo has split along the circumference, but the crack did not propagate through the entire sample.

To approximate the maximum compressive strength of the fiber bundles, the compressive strength of each bamboo sample was plotted against its density. Because the density of bamboo changes with the volume fraction of vascular bundles, and the amount of vascular bundles determines the mechanical properties of the bamboo, density should be an easy-to-measure indicator of the mechanical properties of the bamboo samples. The relationship between density and compressive strength was found to be linear for each four-sample set described above. These plots are shown in Figure 17, and extrapolated in Figure 18.

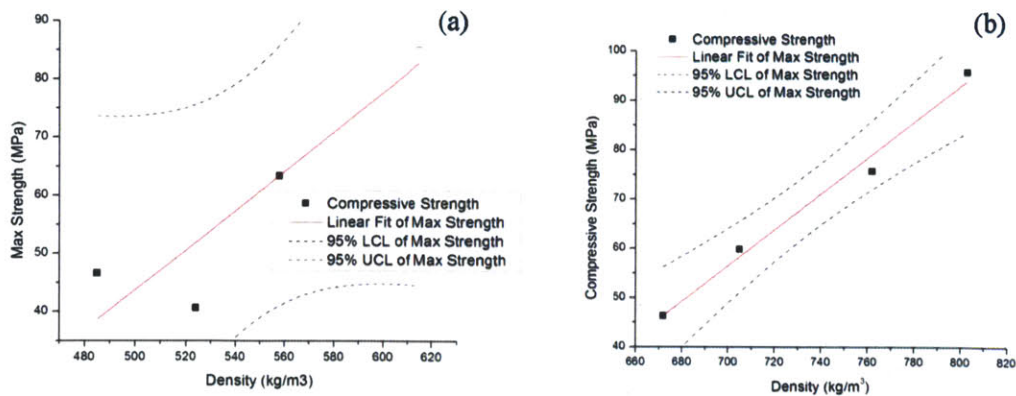


**Fig. 17.** Compressive strength vs. density plots for sets of samples (a) from approximately 15 cm in height and (b) from approximately 115 cm in height.

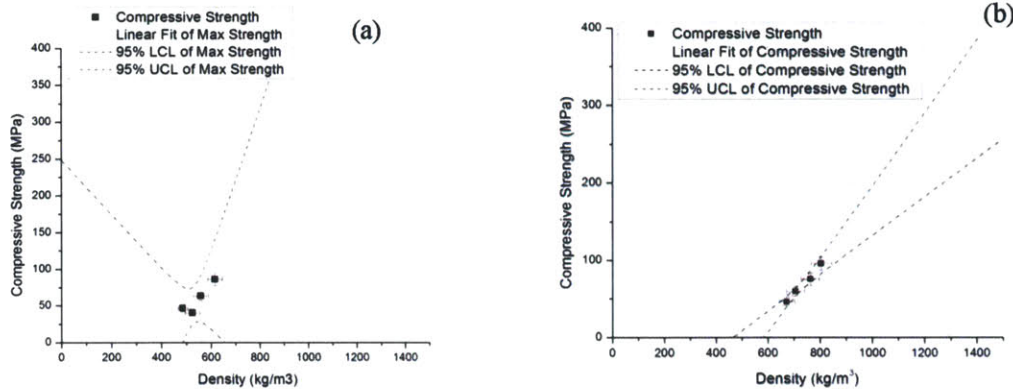


**Fig. 18.** Compressive strength vs. density plots for sets of samples (a) from approximately 15 cm in height and (b) from approximately 115 cm in height, extrapolated to 1500 kg/m<sup>3</sup> density.

The density of the cell walls of wood, which is approximately 80% cellulose, is roughly 1500 kg/m<sup>3</sup> [8,13]. Assuming bamboo fibers to have similar properties to wood, an extrapolation of the data sets above to 1500 kg/m<sup>3</sup> could yield insight as to the compressive strength of the pure fiber. Unfortunately, based on the 95% confidence levels plotted in the graphs above, making an extrapolation to 1500 kg/m<sup>3</sup> on either data set involves much uncertainty, yielding a value of approximately 340 ± 100 MPa.

However, Nogata *et al.* report a density of 1050 kg/m<sup>3</sup> for bamboo fiber [6].

Extrapolating to this density gives a compressive strength of 180 ± 30 MPa, which actually compares well with the hardness values measured for bamboo fiber via nanoindentation. An approximate scaling law common in metals is that the compressive yield strength of a material is equal to its hardness divided by 3:

$$\sigma_y \approx \frac{H}{3}$$

Given hardness values ranging from 390 to 580 MPa as described in section 3.1, a compressive strength of approximately 180 MPa is consistent with this approximate scaling law.

#### **4. Conclusion**

The nanoindentation experiments in this report verify that the mechanical properties of the bamboo fiber do not vary significantly with radial or circumferential position. This is useful knowledge for processing bamboo into a composite structural bamboo product, because the bamboo can be assumed to be axially symmetric. Therefore, any machines designed to process bamboo and form it into a glue-laminated product can be built to take advantage of this symmetry. Furthermore, assuming the mechanical properties of the fibers are constant simplifies the modeling of bamboo as a cellular solid.

The density of bamboo material can be used to predict its compressive strength, a useful metric in designing load-bearing structural components. However, current experiments have only provided useful information over a small range of densities. Further work in this area could include extracting and pressing together bamboo fibers to examine the mechanical properties of more dense bamboo material. These experiments would have the added benefit of revealing more information on how bamboo fibers behave as a composite material in structural bamboo products.



## **5. Acknowledgements**

Many thanks to Professor Gibson and the members of the Cellular Solids Group for giving me the opportunity to conduct research with and learn from them. Thank you as well to Mike Tarkanian and Matt Humbert, whose expertise once again proved invaluable. Thanks to Dr. Alan Schwartzman for his assistance with nanoindentation. Finally, thank you to the Arnold Arboretum for supplying bamboo samples.

## **6. Works Cited**

- [1] Fu, J. “ ‘Moso Bamboo’ in China.” *American Bamboo Society Magazine* **21**(6), December 2000, 12-17
- [2] Paudel, S.K. “Engineered bamboo as a building material.” *Modern Bamboo Structures*. August 2008, 33-40
- [3] Xiao, Y.; Zhou, Q.; and Shan, B. “Design and Construction of Modern Bamboo Bridges.” *Journal of Bridge Engineering* September/October 2010, 533-541
- [4] Chen, G.; Xiao, Y.; Shan, B.; and She, L. Y. “Design and construction of a two-story modern bamboo house.” *Modern Bamboo Structures*, August 2008, 215-221
- [5] Lo, T. Y.; Cui, H.Z.; and Leung, H. C. “The effect of fiber density on strength capacity of bamboo.” *Materials Letters* **58**, 2004, 2595-2598
- [6] Nogata, F.; and Takahashi, H. “Intelligent Functionally Graded Material: Bamboo.” *Composites Engineering* **5**(7), 1996, 743-751
- [7] Gibson, L.J.; and Ashby, M. F. Cellular solids – Structure and properties. Second edition. Cambridge University Press, Cambridge, UK. 1997.
- [8] Gibson, L.J.; Ashby, M.F.; and Harley, B.A. Cellular Materials in Nature and Medicine. Cambridge University Press, Cambridge, UK. 2010.
- [9] Rasband, W.S., “ImageJ,” U. S. National Institutes of Health, Bethesda, Maryland, USA, <http://imagej.nih.gov/ij/>, 1997-2011.
- [10] Oliver, W.C.; Pharr, G.M. “Measurement of hardness and elastic modulus by instrumented indentation: Advances in understanding and refinements to methodology.” *Journal of Materials Research* **19**(1), Jan 2004
- [11] Yu, Yan *et al.* “Cell-Wall Mechanical Properties of Bamboo Investigated by In-Situ Imaging Nanoindentation.” *Wood and Fiber Science*, **39**(4), 2007, 527-535
- [12] Rao, K. M. M., and Rao, K. M. “Extraction and tensile properties of natural fibers: Vakka, date and bamboo.” *Composite Structures*, **77**, 2005, 288-295
- [13] Bodig, J.; and Jayne, B.A. Mechanics of Wood and Wood Composites. Van Nostrand Reinhold Company, New York, NY. 1982.